

Article

Colorimetric and Label-Free Optical Detection of Pb²⁺ Ions via Colloidal Gold Nanoparticles

Jasmin A Flowers ^{1,#}, Monique J Farrell ^{2,#}, Gugu Rutherford ^{3,#} and Aswini K Pradhan ^{4,*,#}¹ Boston Scientific, Maple Grove, Minnesota, USA; jasminflowers24@gmail.com² FTL at Northrop Grumman, Washington, District of Columbia, USA; monique.j.farrell@gmail.com³ NASA Langley Research Ctr, Langley Blvd, Hampton, VA 23681, USA; gugu.n.rutherford@nasa.gov⁴ Department of Physics, Hampton University, Hampton, VA 23668, USA

Research performed at the Center for Materials Research, Norfolk State University, 700 Park Ave., Norfolk, VA 23504, USA

* Corresponding: aswini.pradhan@hamptonu.edu

Abstract: The detection of Lead (Pb) heavy metal in water is crucial in many chemical processes as it is associated with serious health hazard. Here, we report the selective and precise colorimetric detection of Pb²⁺ ions in water exploiting the mechanisms of aggregation and self-assembly of Glutathione (GSH) functionalized gold nanoparticles (GNPs). The carboxyl functional groups are available to create coordination complexes with Pb²⁺ inducing aggregation amongst the GSH-GNPs in the presence of Pb²⁺ due to the chelation of the GSH ligands. The resulting aggregation of amongst the GSH-GNPs in the presence of Pb²⁺ increases the aggregate size depending on available Pb²⁺ ions affecting the plasmonic coupling. This causes in a substantial shift in the plasmon wavelength to a longer wavelength side with increasing Pb²⁺ concentration, resulting in a red-to-blue colorimetric or visual change, enabling instant determination of lead content in water.

Citation: Flowers, J.A.; Farrell, M.J.; Rutherford, G.; Pradhan, A.K. Colorimetric and Label-Free Optical Detection of Pb²⁺ Ions via Colloidal Gold Nanoparticles. *Biosensors* **2022**, *11*, x. <https://doi.org/10.3390/xxxxxx>

Received: date
Accepted: date
Published: date

Publisher's Note: MDPI stays neutral with regard to jurisdictional claims in published maps and institutional affiliations.



Copyright: © 2022 by the authors. Submitted for possible open access publication under the terms and conditions of the Creative Commons Attribution (CC BY) license (<https://creativecommons.org/licenses/by/4.0/>).

Keywords: Gold nanoparticles; surface plasmons; calorimetric detection of metal ions

1. Introduction

Lead metal has caused extensive contamination and health problems in many parts of the world as it is extremely harmful to the environment and severely detrimental to human beings even in low concentrations. It is a cumulative toxin that affects multiple body systems [1]. Specifically, due to bioaccumulation over time, even low concentrations of lead can have serious health effects, such as neurodevelopmental and IQ deficits in children and elevated blood pressure, kidney problems, and infertility in adults [2]. Acute exposures have the ability to cause death as a result from body system damages or disturbances [1]. The disaster of Pb contamination was seen in the city water of Flint, Michigan (called poison in the water) due to hazardous waste disposal in local river water [3–5].

To date, the Environmental Protection Agency (EPA) of the United States and various companies use analytical techniques to test for lead, such as atomic absorption spectrometry, inductively coupled plasma atomic emission spectrometry, and differential pulse anodic stripping voltammetry due to their ability to provide low limits of detection around 1ppb [5]. Unfortunately, these techniques, though highly sensitive, are also extremely sophisticated, costly, and, therefore, are not easily accessible all around the world. They require highly skilled analysts who are capable of operating the bulky equipment. Another downside is these sophisticated analytical techniques are not suitable for on-site applications, which increases the amount of time it takes to receive results. Developing a detection method that is quick, simple, cheap, and sufficiently sensitive would meet the

great demand around the world as well as replace the current conventional analytical methods.

This work presents the capability of lead detection exploiting the mechanisms of aggregation and self-assembly of GSH-GNPs. For the past decade, the field of environmental monitoring has seen the application of nanoparticles, specifically gold, being utilized as functional probes for analyzing toxins, metal ions, and inorganic and organic pollutants [6,7]. Exploiting the properties of GNPs as functional probes provides the capability to use them both as a colloidal and substrate-based sensor. Providing a quick and simplistic detection system could allow worldwide the ability to test water, even in remote locations, to determine its viability. Using GNP probes as a basis for this detection method shows promise, which is presented in this work. We demonstrate a simple, quick, and selective colloidal colorimetric detection method for Pb^{2+} using highly stable, GSH-functionalized GNPs approximately as small as 15nm in diameter.

2. Procedure and Methodology

The procedure for GNP synthesis for this work was based on a more recent method by Graber *et al.* [8,9] due to the simple, quick, and cheap synthesis. The materials used were gold (III) chloride trihydrate, barium chloride, copper (II) sulfate anhydrous, and cadmium acetate hydrate purchased from Sigma Aldrich. Sodium citrate, iron (II) chloride tetrahydrate, nickel (II) acetate hydrate, manganese (II) acetate anhydrous, zinc acetate anhydrous, calcium nitrate tetrahydrate, cobalt (II) acetate tetrahydrate, chromium (III) nitrate nonahydrate, and magnesium fluoride purchased from Alfa Aesar. L-glutathione high purity grade was obtained from Amresco. All chemicals were used without further purification and were diluted using ultra-pure Millipore water ($>18M\Omega$) and deionized (D.I.) water. All glassware was cleaned vigorously with 3.5M HCl, rinsed with copious amounts of milli-Q water, and allowed to dry before use.

The GNPs were synthesized via a quick and simple hot injection method. Approximately, 1mM gold (III) chloride trihydrate solution was made by dissolving 40mg in 100mL of water. It is noted that the GNPs were synthesized with D.I. water and with milli-Q water to compare. This was allowed to heat to approximately 100 °C while stirring. Once it reached a low boil a 39mM sodium citrate (115mg, 10mL of water) solution was added. The solution was allowed to stir for 10 minutes, resulting in a color change from pale yellow to dark red wine color. After 10 minutes, the reaction was quenched by placing the beaker in an ice bath for 5 minutes while swirling the solution. To increase the working volume as well as aid in the cooling process, the solution was diluted 1:1, resulting in 200 mL of GNPs. To modify the surface of the GNPs, we chose glutathione (GSH) as our receptive ligand for Pb^{2+} detection. Using milli-Q water as the solvent 19mM GSH was made. To functionalize the GNPs, we briefly added 100 μ L of 19mM GSH to 800 μ L GNPs in a PMMA cuvette at room temperature. GSH is a non-protein tripeptide made up of cysteine, glycine, and glutamate amino acids. It is cheap, making it a very attractive candidate for surface and electrode modification and for the synthesis of monolayer-protected nanoparticles. The thiol group stemming from the cysteine amino acid has a high affinity towards metals [10,11], in particular gold, resulting in the S-Au covalent bond formation [12]. After the addition of GSH to freshly prepared citrate-stabilized GNPs, their surfaces can be modified by GSH through the aforementioned S-Au covalent bond. GSH has two free $-COOH$ groups and a $-NH^2$ group to provide a hydrophilic interface and a handle for further reactivity with heavy metal ions [13]. At pH 8, the $-NH^2$ group is protonated to $-NH^{3+}$ and, as a result, $-COO^-$ is the only binding site which is known to bind strongly to Pb^{2+} [14]. Metal ions like Fe^{2+} , Cd^{2+} , and Zn^{2+} have been known to bind to the amino group in GSH, thus encouraging a pH of 8, where the amino group is made unavailable and the $-COO^-$ available for binding [14]. Incorporating the resulting zwitterionic form makes our system ideal for Pb^{2+} detection. To functionalize the GNPs, 100 μ L of 19mM GSH was added to 800 μ L GNPs at room temperature in the cuvette. After

functionalized with GSH, the GNPs' aggregation behavior in the presence of Pb^{2+} at room temperature was monitored.

The experimental trials were created by adding 900 μL of GSH-GNPs and 120 μL of 1M NaCl to 120 μL of the varying concentrations of Pb^{2+} . After addition, the solution was sufficiently mixed via pipetting in a cuvette. At high ionic strength, the Pb^{2+} induced an immediate color change from red to blue which corresponded to changes in absorbance. This change in absorbance was measured using a LAMBDA 950 UV/Vis/NIR spectrometer by PerkinElmer. A time-study was conducted from 0-60 minutes for each concentration of Pb^{2+} to monitor the progression of aggregation over time. The selectivity of the system for Pb over various other metal ions (Fe^{2+} , Zn^{2+} , Ba^{2+} , Ni^{2+} , Ca^{2+} , Cr^{3+} , Mg^{2+} , Mn^{2+} , Cu^{2+} , and Cd^{2+}) was investigated under the same conditions as previously stated. 100 μM of each metal ion was tested and compared to 50 μM of Pb^{2+} . SPR magnitude changes were investigated when initially mixed and after 10 minutes of incubation.

3. Results and Discussion

In the presence of Pb^{2+} , GSH-GNPs undergo aggregation due to the formation of a chelating complex [15]. After GSH-functionalization of the GNPs, the carboxyl functional groups are available to create coordination complexes with Pb^{2+} . These coordination bonds are what induce aggregation amongst the GSH-GNPs in the presence of Pb^{2+} due to the chelation of the GSH ligands [10,11]. Due to this mechanism of particle-particle coupling or plasmonic coupling, a substantial shift in the plasmon band energy to a longer wavelength occurs, resulting in a red-to-blue color change.

The shorter wavelengths, corresponding to high energy, of light are only able to excite the localized SPR of the smaller GNPs and the longer wavelengths, corresponding to low energy, of light are able to excite the localized SPR of the larger GNPs. Therefore, small GNPs absorb shorter wavelengths, whereas large GNPs absorb longer wavelengths. This explains the shift of the SPR band to the right as the GNPs grow in size, resulting in the change of color from red to blue. When the GNPs aggregate, the distance between each particle decreases. This is where near-field coupling begins to dominate and produces a strong enhancement of the localized electric field within the inter-particle spacing. Those enhanced electronic fields are confined within a very small space spanning the circumference of the GNPs and decay exponentially [17,18]. This mechanism proves highly beneficial because it exploits the local SPRs found on spherical nanoparticles to detect Pb^{2+} due to the change in the energy of the GNPs.

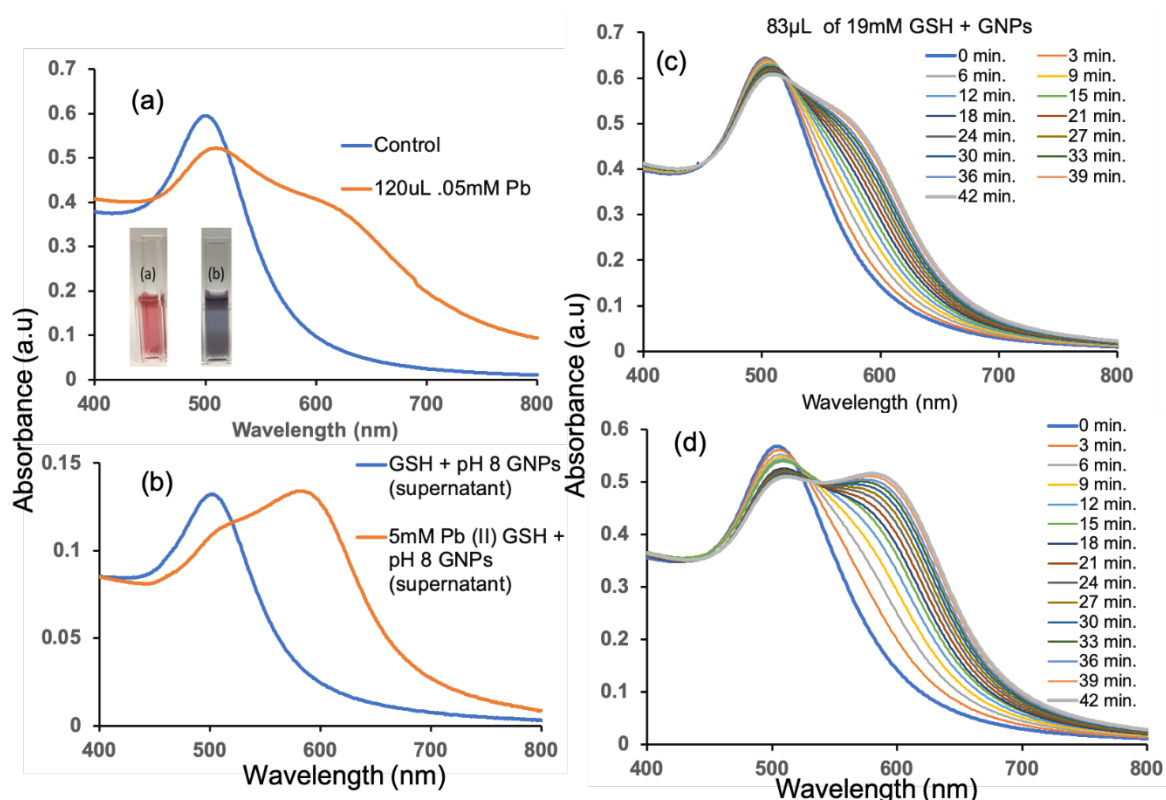


Figure 1. (a) UV-Vis spectra and pictures of the GSH-GNPs in the (a) absence and (b) presence of 0.05 mM Pb²⁺ of supernatant solutions of pH 8 and GSH-GNPs with and without addition of 5 mM Pb²⁺, (c) UV-Vis spectra of 83 μL of 19 mM GSH added to GNPs to make up the control investigated over 42 minutes and (d) UV-Vis spectra of 0.05 mM Pb²⁺ added to GSH-GNPs over a 42 min time-frame.

A substantial shift in the plasmon band energy to a longer wavelength occurs, resulting in a red-to-blue color change as exhibited in Fig. 1 (a) and (b) for the presence of 0.05 mM Pb²⁺ of supernatant solutions of pH 8 and GSH-GNPs with and without addition of 5 mM Pb²⁺. Fig. 1 (c) and (d) shows the UV-Vis spectra of 83 μL of 19 mM GSH added to GNPs to make up the control investigated over 42 minutes and for 0.05 mM Pb²⁺ added to GSH-GNPs over a 42 min timeframe. Using the cleaned system, we employed a similar visual detection to determine the cleaned system's capability to detect Pb²⁺. There have been reports [19] based upon the rate of aggregation in the presence of Pb²⁺ due to an unstable control. Though our control was aggregating at a similar rate be Pb²⁺ was added, we were unable to reach the same concentration sensitivity. Therefore, we explored ways to stabilize our control by altering our GSH solution and achieve a sufficient Pb²⁺ concentration sensitivity. First, we changed the amount of GSH used to functionalize the GNPs by reducing the volume of set concentration added to the 800 μL of GNPs. As expected, the lesser the volume of GSH added, the more visually stable the control seemed. This is probably in-part due to the pH of the GSH and the GNPs, 2.93 and 5.8, respectively. At an acidic pH, the functional groups of GSH are highly protonated, creating an overall positively charged molecule which is attracted to the negatively charged surface of the GNPs. The less GSH molecule means the less ligands to bind multiple GNPs together, ultimately meaning less aggregation or a slower rate of aggregation for the control. The volumes tested were, 50, 60, 70, 80, 85, and 90 μL of 19 mM GSH. We noticed slight color change with 85 μL and no color change with 80 μL immediately upon addition. With this in mind, 83 μL of 19 mM GSH was used to investigate the new control stability with a 42-minute time-study with measurements taken every 3 minutes, Fig. 1 (c). This still did not provide the stable control we desired as seen in the broadening and shifting of the SPR peaks in the absorbance spectra indicative of aggregation and color change. Though the control

was not ideal, we proceeded with the Pb^{2+} detection investigation to determine the control's potential. A 42-minute time-study with 0.05mM Pb^{2+} (Fig. 1(d)) and a 20-hour time drive absorbance study of the control and the lowest Pb^{2+} concentration, .00001mM Pb^{2+} . Similar to that of Zhong et al [19] we investigated our control's ability to detect Pb^{2+} based on the rate of aggregation. It produced a control that changed from red to purple within 10 minutes. When Pb^{2+} was added, a quicker rate of aggregation was noticed within the 10 minute time-frame from red to blue. With this mechanism in mind, we sought to determine if we had achieved a similar aggregation rate, but within a longer timeframe.

With a stable control and the colorimetric detection of Pb^{2+} ensued, we evaluated the detectable minimum concentration of Pb^{2+} in aqueous solution by color change. We added the Pb^{2+} with concentrations of 5-0.00001mM into the control Figs. 2 (a)-(b) show images for the decreasing concentrations of Pb^{2+} at 0 minutes and 60 minutes. The lower concentrations (0.0005mM, 0.0001mM, 0.00005mM, and 0.00001mM) do not follow the assumed trend. That is as the concentration of Pb^{2+} decreases, we expect the peak width to decrease and revert back to the characteristic magnitude of the control. However, it does not, and it indicates that the system is not able to properly discriminate between the low concentrations using UV-vis as a characterization method. They report limits of detection (LOD) from 20 ppb [13] to an audacious 100 ppt [15]. However, they were not able to show visual detection at such low concentrations. Further optimization of this system with the goal of true visual detection of lower concentrations of Pb^{2+} would create the possibility of a competitive system that is quick and simple to make and detects trace levels of Pb^{2+} within 10 minutes.

A clear size distribution of the GSH-GNPs between 500-5000nm is observed in the presence of Pb^{2+} as shown in Fig. (c) to (f). Beqa et al. [15] reported a GNP-based simple colorimetric and ultrasensitive DLS Assay for the selective detection of Pb^{2+} . They reported sensitivity down to 100ppt using DLS as their qualitative method of detection. Visually, however, they were only able to see a color change down to 1ppm. Upon further optimization of our system, it is expected that we will see comparable results to that reported one. In addition to this, we provide a much better GNP synthesis method in terms of speed and stability of the product as well as a faster detection timeframe.

It is clear that as the volume of Pb^{2+} increases, the SPR peak has a change attributed to the coupled plasmon absorbance of the GNPs in close contact. As the light in the UV-vis passes through the cuvette containing the solution, some is absorbed, and some is transmitted. The larger particle sizes within the solution correspond to longer wavelengths due to the changes made in the localized SPRs. This is why we observe the broadened and shifted absorbance peaks. FESEM images help explain this visually. Fig. 2 (e)-(f) shows images of GNPs as-synthesized, functionalized with GSH, 1M NaCl added to GSH-GNPs, and in the presence of Pb^{2+} . The large aggregates cause a change in the localized SPRs of the individual GNPs due to coupling as well as the overall energy of the aggregate, which is reflected in the corresponding absorbance spectra. This large size correlates to the blue color we see in the system in the presence of Pb^{2+} . Based on the obtained images from FESEM, the size of the as-synthesized D.I. GNPs averaged around 15 nm. This corresponds to the 500 nm absorbance wavelength characteristic of their SPR. As previously explained, the smaller size and consistency in shape of the GNPs correlate to lower wavelengths in the absorbance spectra. From this, we can confirm the synthesis of high energy, uniform spherical GNPs monodispersed in solution.

A clear size distribution of the GSH-GNPs between 500-5000nm is observed in the presence of Pb^{2+} as shown in Fig. (c) to (f). Beqa et al. [15] reported a GNP-based simple colorimetric and ultrasensitive DLS Assay for the selective detection of Pb^{2+} . They reported sensitivity down to 100ppt using DLS as their qualitative method of detection. Visually, however, they were only able to see a color change down to 1ppm. Upon further optimization of our system, it is expected that we will see comparable results to that reported one. In addition to this, we provide a much better GNP synthesis method in terms of speed and stability of the product as well as a faster detection timeframe.

It is clear that as the volume of Pb^{2+} increases, the SPR peak has a change attributed to the coupled plasmon absorbance of the GNPs in close contact. As the light in the UV-vis passes through the cuvette containing the solution, some is absorbed, and some is transmitted. The larger particle sizes within the solution correspond to longer wavelengths due to the changes made in the localized SPRs. This is why we observe the broadened and shifted absorbance peaks. FESEM images help explain this visually. Fig. 2 (e)-(f) shows images of GNPs as-synthesized, functionalized with GSH, 1M NaCl added to GSH-GNPs, and in the presence of Pb^{2+} . The large aggregates cause a change in the localized SPRs of the individual GNPs due to coupling as well as the overall energy of the aggregate, which is reflected in the corresponding absorbance spectra. This large size correlates to the blue color we see in the system in the presence of Pb^{2+} . Based on the obtained images from FESEM, the size of the as-synthesized D.I. GNPs averaged around 15 nm. This corresponds to the 500 nm absorbance wavelength characteristic of their SPR. As previously explained, the smaller size and consistency in shape of the GNPs correlate to lower wavelengths in the absorbance spectra. From this, we can confirm the synthesis of high energy, uniform spherical GNPs monodispersed in solution.

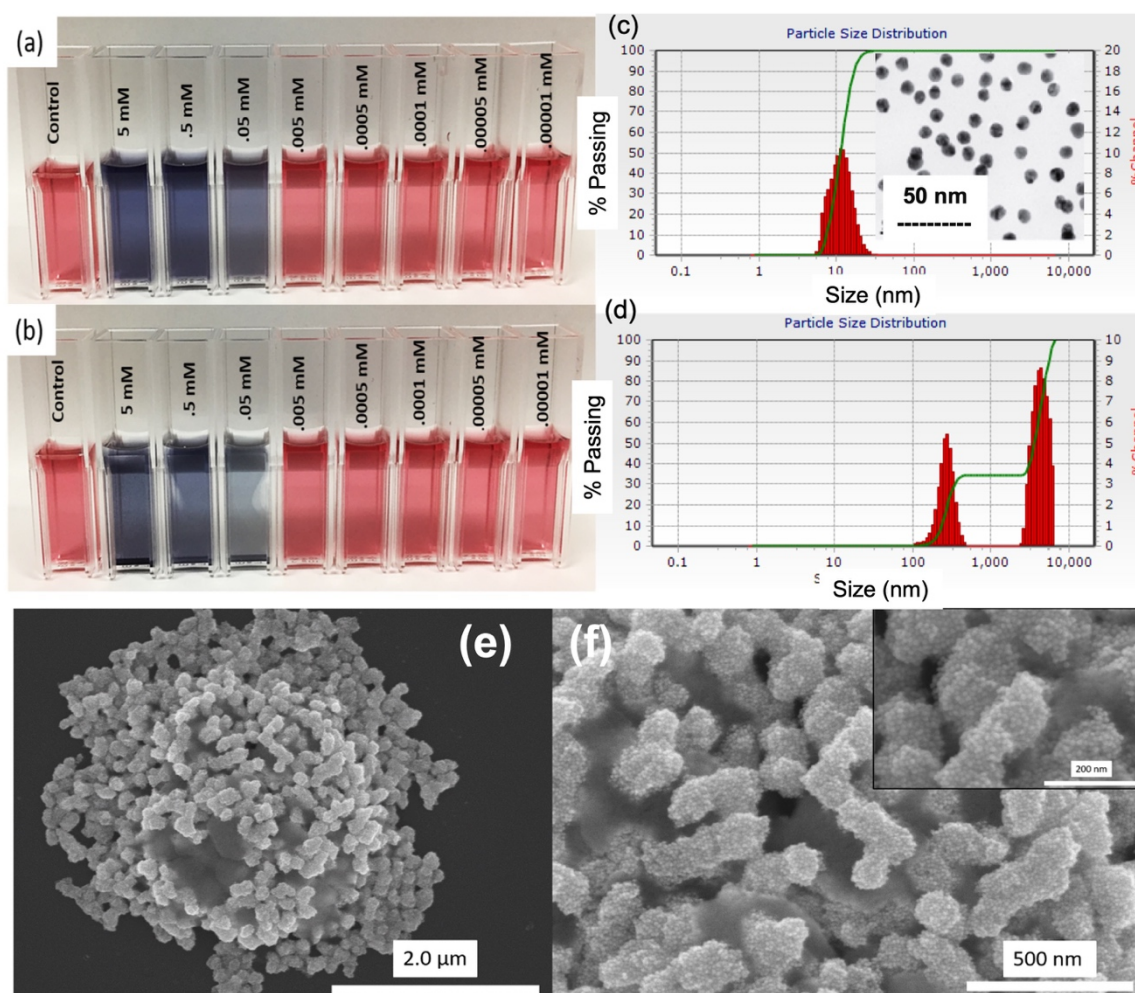


Figure 2. Images of colloidal solutions of GSH-GNPs (a) 0 minute, (b) 60 minutes shots of Pb^{2+} detection at various concentrations. (c) Dynamic light scattering (DLS) data showing particle size distribution of control (Au NPs) before, and (d) after the addition of 120 μ L of 0.05 mM Pb^{2+} . (e) FESEM image of GSH-GNPs aggregation induced by 50 μ M Pb^{2+} , and (f) Enlarge scale of GSH-GNPs aggregation induced by 50 μ M Pb^{2+} . Inset of (c) shows the FESEM image of Au NPs and inset of (f) show the GSH-GNPs aggregation induced by Pb^{2+} ions.

The size and shape of the as-synthesized GNPs create an ideal platform for colorimetric detection of Pb^{2+} due to their high surface area-to-volume ratio. The GNPs' SPR frequency is highly sensitive to the refractive index/dielectric nature of its interface with the environment surrounding it [20]. Changing this environment will also shift the SPR frequency [21,22] thus enabling us to visually detect via colorimetric change. In addition to this, GNPs' large surface area enables them to be modified easily to become probes using thiolated or disulfide modified ligands, electrostatic interaction, antibody-antigen association, and streptavidin-biotin binding as seen in many publications [13,23,24].

The absorbance ratio with respect to time provides further insight into the capabilities of this detection system. Within 10 minutes, our system is able to detect the presence of Pb^{2+} by a quick and clear change in color as reflected in the spectra, Fig. 3 (a) and (b). This provides the user with a rapid detection system using an extremely stable control as a foundation to compare the color change to. The absorbance values of GSH-GNPs upon the addition of 120-40 μ L of .05mM Pb^{2+} reached a maximum at 10 minutes, whereas the values of the other concentrations (30-10 μ L) kept increasing. Upon the addition of 120 μ L of 0.05mM Pb^{2+} , the response completed within seconds, indicating that the aggregation response of GSH-GNPs was highly dependent on the concentration of Pb^{2+} . This result represents the fast performance of this probe for the detection of Pb^{2+} . A visual time-study to see how quickly we can detect Pb^{2+} at the varying concentrations. In Fig. 3(c) we have shown the images depicting the progression of time and volume of .05mM Pb^{2+} from 0 to 10 minutes. Within 10 minutes, this system provides visual proof of its ability to detect 25 μ M Pb^{2+} . Absorbance data provides further insight into the system's capability to detect the lower Pb concentrations.

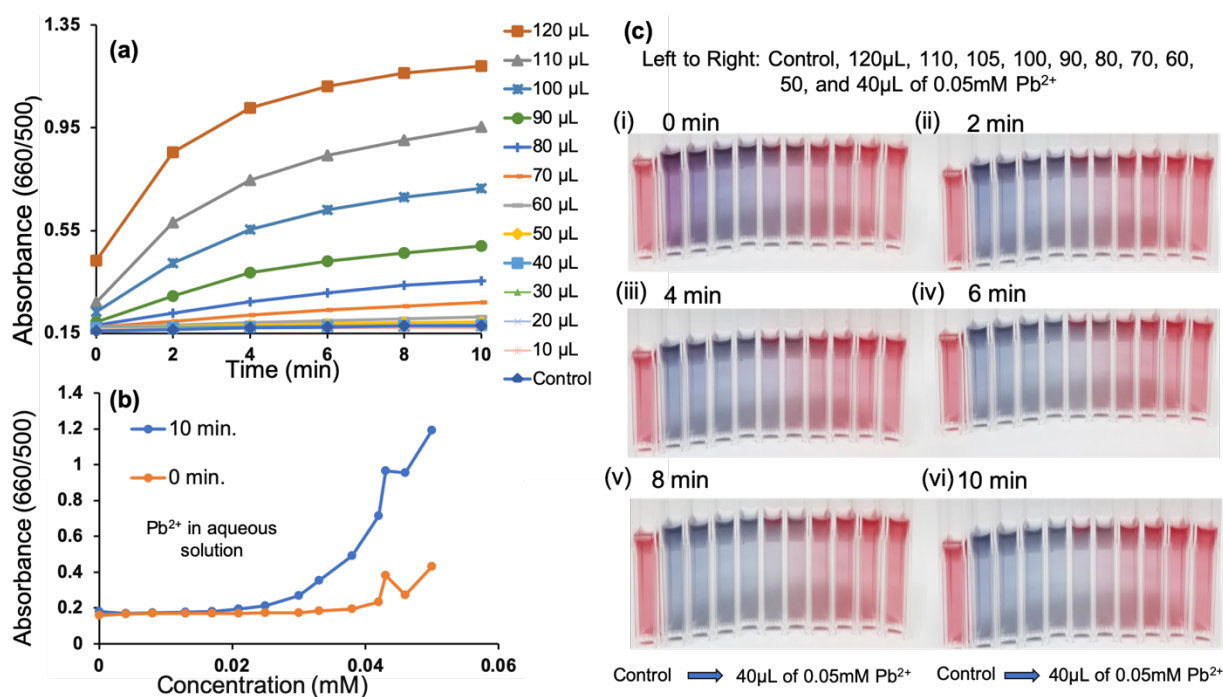


Figure 3. (a) Plots of the time-dependent absorption ratio ($A_{660/500}$) over 10 minutes of various volumes of 0.05mM Pb^{2+} added to the control. (b) $A_{660/500}$ vs various concentrations of Pb^{2+} in the range of 0.004-0.05mM. (c) Images depicting the presence of decreasing volumes of 0.05mM Pb^{2+} solutions at (i) 0 min, (ii) 2 min, (iii) 4 min, (iv) 6 min, (v) 8 min and (vi) 10 min. From Left to right: Control, 120 μ L, 110 μ L, 105 μ L, 100 μ L, 90 μ L, 80 μ L, 70 μ L, 60 μ L, 50 μ L, and 40 μ L of a 0.05mM Pb^{2+} .

Determining the MDC of this system is dependent upon the linear regression of the relationship between the absorbance ratio and concentration. Such a relationship is used as a basis to quantify Pb^{2+} in aqueous solutions. The SPR peaks of the GSH-GNPs at 660

and 500nm are related to the quantities of dispersed and aggregated GSH-GNPs, respectively. Therefore, we used the ratio of the values of absorbance 660/500 ($A_{660/500}$) to express the molar ratio of aggregated and dispersed GSH-GNPs. A linear calibration curve ($R^2=0.737$) was observed from the linear regression of absorbance value versus concentration, Fig. 3 (b). A system exhibiting an R^2 value of .98 or higher would be ideal as it would indicate its ability to quantitatively determine the Pb^{2+} concentration present in the system. From this, we suggest that this probe has the capability to be used for detecting Pb^{2+} , but further optimization is needed in order to use this as a quantifying process.

Several commonly existing metal ions were tested: Fe^{2+} , Zn^{2+} , Ba^{2+} , Ni^{2+} , Ca^{2+} , Cr^{3+} , Mg^{2+} , Mn^{2+} , Cu^{2+} , and Cd^{2+} . The image below (Fig. (a) and (b)) illustrates the GSH-GNPs in the presence of $100\mu M$ of the various metal ions and $50\mu M$ Pb^{2+} . The results demonstrated the other metal ions have no obvious effect on the system as compared to the Pb^{2+} . The Cd^{2+} ion, however, did show a mild effect on the control as shown in Figs. 4 (c)- (e), but nowhere near as much as Pb^{2+} did. However, this technique is also capable of detecting trace amount of Cd^{2+} heavy metal which is only 25% sensitive to Pb^{2+} ions due to poor binding of Cd^{2+} ions to $-COO^-$ binding sites. Absorbance values ($A_{660/500}$) of the control after the addition of the metal ions do not compare to that of the system with Pb^{2+} ions as shown in Fig. 4 (d), detailing the system's high selectivity of Pb^{2+} over various common metals found in water and consistent with the recent report [25]. As GSH has two free $-COOH$ groups (shown as the ends of the Y-shape molecules in the schematics of Fig. 4 (e)) and a $-NH_2$ group to provide a hydrophilic interface and a handle for further reactivity with heavy metal ions. The $-NH_2$ group is protonated to $-NH_3^+$ and, as a result, $-COO^-$ is the only binding site which is known to bind strongly to Pb^{2+} as discussed earlier. Metal ions like Fe^{2+} , Cd^{2+} , and Zn^{2+} have been known to bind to the amino group in GSH, but the amino group is made unavailable.

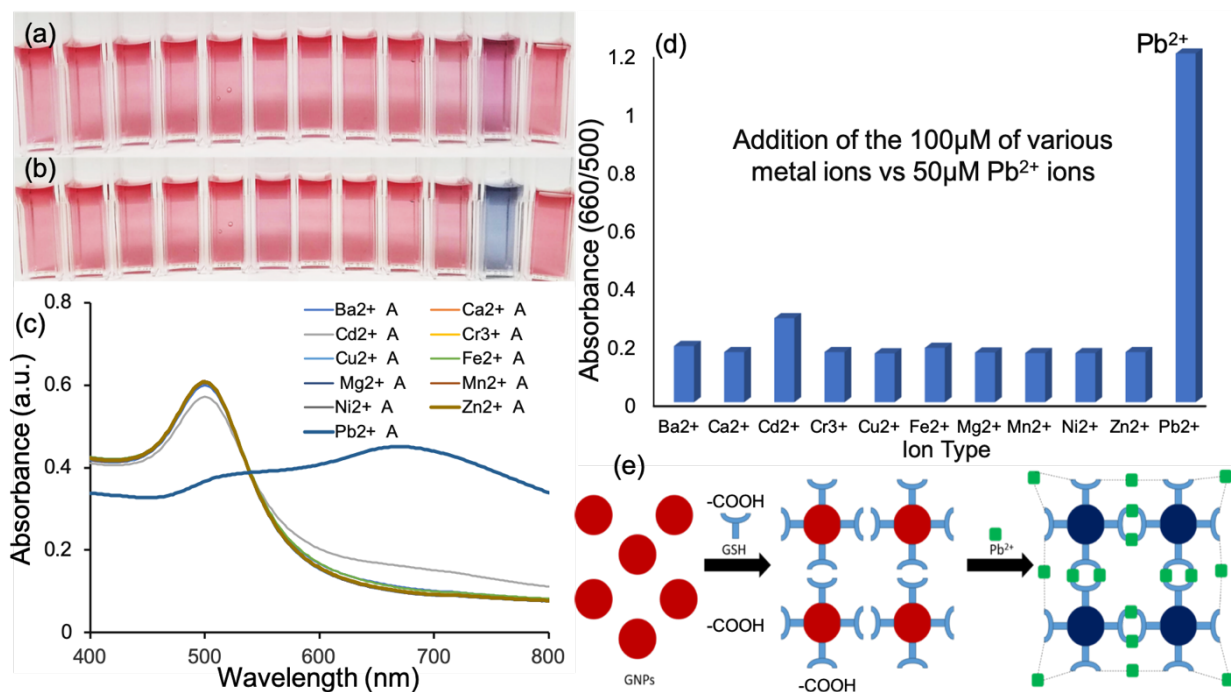


Figure 4. Various ion detection (a) 0 min (b) 10 min. (b). From left to right: $100\mu M$ Fe^{2+} , Zn^{2+} , Ba^{2+} , Ni^{2+} , Ca^{2+} , Cr^{3+} , Mg^{2+} , Mn^{2+} , Cu^{2+} , Cd^{2+} , $50\mu M$ Pb^{2+} , and the control. (c) Absorption spectra comparing control with $100\mu L$ of various metal ions vs $50\mu M$ Pb^{2+} (all metals were incubated with control for 10 minutes). (d) The values absorbance ($A_{660/500}$) of the control upon the addition of the $100\mu M$ of various metal ions vs $50\mu M$ Pb^{2+} ions, and (e) Schematic: Schematic representation of the progression GNP's going through after functionalization with GSH and the detection of Pb^{2+} through the formation of a coordination complex.

4. Summary

we have produced a simple, cost-effective, quick, and portable detection method using GSH-GNP-based colorimetric probe that allows rapid, real-time detection of Pb^{2+} in just 10 minutes. The experimental results show the strength of this system in terms of selectivity and the capability of improvement for sensitivity of Pb^{2+} in aqueous solutions. We believe this method may offer a faster approach for the detection of Pb^{2+} in aqueous biological and environmental samples for practical applications. Our method offers a solid proof-of-concept with proven experiment evidence for a rapid and cost-effective detection of Pb^{2+} toxic pollutants in water.

Author Contributions: Funding acquisition by A.K.P.; J.A.F. conceived and conducted the experiments. M.J.F. and G.R. contributed to experiments. A.K.P. supervised and guided the research. All authors have read and agreed to the published version of the manuscript.

Funding: This work was supported by the National Science Foundation Centers of Research Excellence in Science and Technology (NSF-CREST) Grant Number HRD 1036494 and 1547771, All the funded projects were managed by the Project Director, AKP.

Acknowledgments: We thank Erin A. Jenrette and Kevin Santiago for their experimental help.

Conflicts of Interest: The authors declare no conflict of interest.

References

1. Advisory Committee on Childhood Lead Poisoning Prevention Of the Centers for Disease Control and Prevention, "Guidelines for Measuring Lead in Blood Using Point of Care Instruments," pp. 1–16, **2013**.
2. Lead Action, "Lead Action News." **1993**.
3. CNN, "Flint water crisis fast facts," *CNN Online*, **2016**.
4. Anon, "Lead and Copper Rule, Drinking Water Requirements for States and Public Water Systems "US EPA," **2008**. Available: file:///E:/School Work/Environment Analysis/Assignment 1/Bio-geochemical Cycles and Transfer of Substances in Ecosystems/References/Lead and Copper Rule Drinking Water Requirements for States and Public Water Systems US EPA.html.
5. United States Environmental Protection Agency Office of Water, "Analytical Methods Approved for Drinking Water Compliance Monitoring of Inorganic Contaminants and Other Inorganic Constituents Alkalinity Method Organization Reference Title Date EPA Publication Number Source of Method," September, **2016**.
6. Cheon, J.; and Lee, J. H. "Synergistically integrated nanoparticles as multimodal probes for nanobiotechnology," *Acc. Chem. Res.*, **2008**, 41, 1630.
7. Wang, Z.; and Ma, L. "Gold nanoparticle probes," *Coord. Chem. Rev.*, **2009**, 253, 1607.
8. Graber, K.C; et al.,*J. Annal of Chem.***1997**, 69,471.
9. Sardar, R.; Funston, A. M.; Mulvaney, P.; and Murray, R. W. "Gold nanoparticles: Past, present, and future," *Langmuir*, **2009**, 25, 13840.
10. Sheng, C.; Zhao, H.; Gu, F.; and Yang, H. "Effect of Pb^{2+} on L-glutathione monolayers on a silver surface investigated by surface-enhanced Raman scattering spectroscopy," *J. Raman Spectrosc.*, **2009**, 40, 1274.
11. Christopher, J.; et al., "Formation and structure of self-assembled monolayers of alkanethiolates on palladium," *J. Am. Chem. Soc.* **2003**, 125, 2597.
12. Ulman, A. "Formation and Structure of Self-Assembled Monolayers," *Chem. Rev.*, **1996**, 96, 1533.
13. Chai, F.; Wang, C.; Wang, T.; Li, L.; and Su, Z. "Colorimetric detection of Pb^{2+} using glutathione functionalized gold

- nanoparticles,” *ACS Appl. Mater. Interfaces*, **2010**, *2*, 1466.
14. Kim, I.B.; Dunkhorst, A.; Gilbert, J.; and Bunz, U. H. F. “Sensing of lead ions by a carboxylate-substituted PPE: Multivalency effects,” *Macromolecules*, **2005**, *38*, 4560.
 15. Beqa, L.; et al., “Gold nanoparticle-based simple colorimetric and ultrasensitive dynamic light scattering assay for the selective detection of Pb(II) from paints, plastics, and water samples,” *ACS Appl. Mater. Interfaces*, **2011**, *3*, 668.
 16. Mao, X.; Li, Z. P.; and Tang, Z. Y. “One pot synthesis of monodispersed L-glutathione stabilized gold nanoparticles for the detection of Pb²⁺ ions,” *Front. Mater. Sci.*, **2011**, *5*, 322.
 17. Gunnarsson L.; et al., “Confined plasmons in nanofabricated single silver particle pairs: Experimental observations of strong interparticle interactions,” *J. Phys. Chem. B*, **2005**, *109*, 1079.
 18. Su, K. H.; et al., “Interparticle coupling effects on plasmon resonances of nanogold particles,” *Nano Lett.* **2003**, *3*, 1087.
 19. Zhong, G.; Liu, J.; and Liu X. “A fast colourimetric assay for lead detection using label-free gold nanoparticles (AuNPs),” *Micromachines*, **2015**, *6*, 462.
 20. Stewart, M. E.; et al., “Nanostructured plasmonic sensors,” *Chem. Rev.* **2008**, *108*, 494.
 21. Niemeyer C. M.; and Simon, U. “DNA-based assembly of metal nanoparticles,” *Eur. J. Inorg. Chem.* **2005**, *18*, 3641.
 22. Yu, C.; and Irudayaraj, J. “Multiplex biosensor using gold nanorods,” *Anal. Chem.*, **2007**, *79*, 572.
 23. Rutherford G. et al., “Photochemical Growth of Highly Densely Packed Gold Nanoparticle Films for Biomedical Diagnostics,” *ECS J. Solid State Sci. Technol.*, **2015**, *4*, S3071.
 24. Farrell, M. J.; Rutherford, G. N.; and Pradhan, A. K. “Characterization of the Effects of 3-Aminopropyl Triethoxysilane on Stability, Optical Properties and Morphology of Colloidal Gold Nanoparticles,” *Curr. Phys. Chem.*, **2016**, *6*, 145.
 25. E. Priyadarshini, E.; and Pradhan, E. “Metal-induced aggregation of valine capped gold nanoparticles: An efficient and rapid approach for colorimetric detection of Pb²⁺ ions”, *Scientific Reports*, **2017**, *7*, 9278.